

Diffuse γ -rays and \bar{p} flux from dark matter annihilation — a model for consistent results with EGRET and cosmic ray data

Xiao-Jun Bi^{1,2,*}, Juan Zhang¹, and Qiang Yuan¹

¹ *Key laboratory of particle astrophysics, IHEP,*

Chinese Academy of Sciences, Beijing 100049, P. R. China

² *Center for High Energy Physics, Peking University, Beijing 100871, P. R. China*

Abstract

In this work we develop a new propagation model for the Galactic cosmic rays based on the GALPROP code, including contributions from dark matter annihilation. Its predictions of the Galactic diffuse γ ray spectra are compatible with the EGRET data in all sky regions. It also gives consistent results about the diffuse γ ray longitude and latitude distributions. The B/C, $^{10}\text{Be}/^9\text{Be}$, proton, electron and antiproton spectra are in agreement with cosmic ray measurements as well. In this model we have taken a universal proton spectrum throughout the Galaxy without introducing large fluctuation, considering the proton energy loss is negligible. The dark matter annihilation signals are “boosted” after taking the contributions from subhalos into account. Another interesting feature of this model is that it gives better description of the diffuse γ rays when taking the source distribution compatible with supernova remnants data, which is different from previous studies.

*Electronic address: bixj@mail.ihep.ac.cn

I. INTRODUCTION

Cosmic ray (CR) propagation is a complex process involving diffusion by magnetic field, energy losses and spallation by interactions with the interstellar medium (ISM). Diffuse Galactic γ -rays are produced via the decay of neutral pion and kaon, which are generated by high energy cosmic nuclei interacting with interstellar gas, and via energetic electron inverse Compton (IC) scattering and bremsstrahlung. The γ rays are not deflected by the magnetic field and the ISM is transparent to γ -rays below a few TeV [1]. Therefore, the observation of the diffuse γ -ray spectra and distribution is a valuable diagnosis of the self-consistency of propagation models, the distribution of CR sources and the ISM. The Galactic diffuse γ rays has been measured by EGRET [2, 3] and exhibits an excess above ~ 1 GeV compared to prediction [3]. The theoretical calculations are based on a conventional CR model, whose nuclei and electron spectra in the whole Galaxy are taken to be the same as those observed locally.

The discrepancy has attracted much attention [4, 5, 6, 7, 8, 9, 10] since it was first raised. It may either indicate a non-ubiquitous proton or electron spectrum, or the existence of new exotic sources of diffuse γ -ray emission.

Many efforts have been made to solve the “GeV excess” problem within the frame of CR physics, such as adopting different CR spectra [4, 5, 6], or assuming more important contribution to diffuse γ -rays from CR sources [7]. A brief review of these efforts is given in [6]. In that paper an “optimized” propagation model has been built by directly fitting the observed diffuse γ -ray spectrum. This “optimized” model introduces interstellar electron and proton intensities that are different from the local ones and reproduces all the CR observational data at the same time. Up to now, it seems to be the best model to explain the EGRET diffuse γ -ray data based on CR physics. However, this “optimized” model is fine tuned by adjusting the electron and proton injection spectra, while keeping the injection spectra of heavier nuclei unchanged, as in the conventional model, so that the B/C ratio is not upset. Furthermore a large scale proton spectrum different from the locally measured one might not be reasonable, since the proton diffusion time scale is much smaller than its energy loss time scale, which tends to result in a large scale universal proton spectrum within the Galaxy apart from some specific sources. Unlike protons, the electron spectrum may have large spatial fluctuation due to their fast energy losses from IC, bremsstrahlung,

ionization and the stochastic sources [11].

Another interesting solution, given by de Boer et al. [8, 9, 10], is that the “GeV excess” is attributed to dark matter (DM) annihilation from the Galactic halo, where the DM candidate is the neutralino from the supersymmetry (SUSY). By fitting both the background spectrum shape from cosmic nuclei collisions and the signal spectrum shape from dark matter annihilation (DMA) they found the EGRET data could be well explained [8]. This suggestion is very interesting and impressive, due to the fact that in 180 independent sky regions¹, all the discrepancies between data and the standard theoretical prediction can be well explained by a single spectrum from DMA with $m_\chi = 50 \sim 70$ GeV. Furthermore, by fitting the spatial distribution of the diffuse γ -ray emission they reconstructed the DM profile, with two rings supplemented to the smooth halo. The ring structure seems also necessary to explain the damping in the Milky Way rotation curve [8] and the gas flaring [10]. However, the DMA solution to the “GeV excess” also meets a great challenge because of its prediction of the antiproton flux. In de Boer’s model, this flux is more than one order of magnitude greater than data [12]. The overproduction of antiprotons comes from two factors: a universal “boost factor” ~ 100 of the diffuse γ -rays boosts the local antiproton flux by the same amount; the two rings introduced to account for the diffuse γ -ray flux enhance the antiproton flux greatly since they are near the solar system and are strong antiproton sources. In their work, de Boer et al. did not try to develop a propagation model. Instead they focused on *reconstruction* of the DM profile by fitting the EGRET data. They need a “boost factor” to enhance the contribution from DMA. The background contribution from pion decay is arbitrarily normalized in order to fit data best.

In the present work we try to build a propagation model to explain the EGRET diffuse γ -ray data based on both Strong’s and de Boer’s models while overcoming their difficulties. In our model the diffuse γ -ray comes from both CRs and DMA directly. On one hand we do not introduce a different interstellar proton spectrum from the local one; on the other our model gives consistent \bar{p} flux even when including contribution from DMA. Furthermore we do not need the large “boost factor” to DMA or renormalization factor to CR contribution. Actually, the γ -ray flux from DMA is boosted by taking the subhalos into account. The

¹ The division at low energies may be problematic as the EGRET point spread function is about 6° and non-Gaussian at low energy.

diffuse γ -ray spectra at different sky regions and its profiles as functions of Galactic longitude and latitude are well consistent with EGRET data. In a previous paper [13], we have briefly introduced our model. Full details are given in the present paper.

The paper is organized as follows. We describe the calculation of the DMA contribution in Section II. In Section III, we focus on the conventional CR model. As underlined, it explains the EGRET data, but produces too large \bar{p} flux. In Section IV, we present our new propagation model and its predictions for the diffuse γ -ray spectra and profiles, and the \bar{p} flux. Finally we summarize and conclude in Section V.

II. DARK MATTER ANNIHILATION

Here, we calculate the diffuse γ -ray flux from DMA. The frame of minimal supersymmetric extension of the standard model (MSSM) is retained, where we assume that DM consists of the lightest neutralinos. A pair of neutralinos in the Galactic halo can annihilate into leptons, quarks and gauge bosons. Their decay products include a γ -ray continuum and thus contribute to the γ -rays diffuse emission produced by CR interaction with the ISM.

A. Particle factor

The flux of γ rays from the neutralino annihilation is given by

$$\Phi(E) = \frac{\langle\sigma v\rangle}{2m_\chi^2} \frac{dN}{dE} \int dV \frac{\rho^2}{4\pi d^2} = \frac{1}{4\pi} \frac{\langle\sigma v\rangle}{2m_\chi^2} \frac{dN}{dE} \times \frac{1}{d^2} \int \rho^2(r) r^2 dr d\Omega, \quad (1)$$

where $\langle\sigma v\rangle$ is the averaged neutralino annihilation cross section times relative velocity, $\frac{dN}{dE}$ is the differential flux in a single annihilation, m_χ is the mass of neutralino, d is the distance between the detector and the γ -ray source, and $\rho(r)$ is the spherically-averaged DM distribution, determined by numerical simulation or by observations. The flux in Eq. (1) is determined by two independent factors, the first one only depending on the DM particle nature (mass, strength of interaction and so on), the second one depending on the DM distribution only. The first factor is denoted as “particle factor” and the second as “astrophysics factor”.

The “particle factor” is calculated by doing a random scan in the SUSY parameter space and choosing models which could satisfy all the collider and cosmological constraints. However, there are more than one hundred free SUSY breaking parameters, even for the R-parity

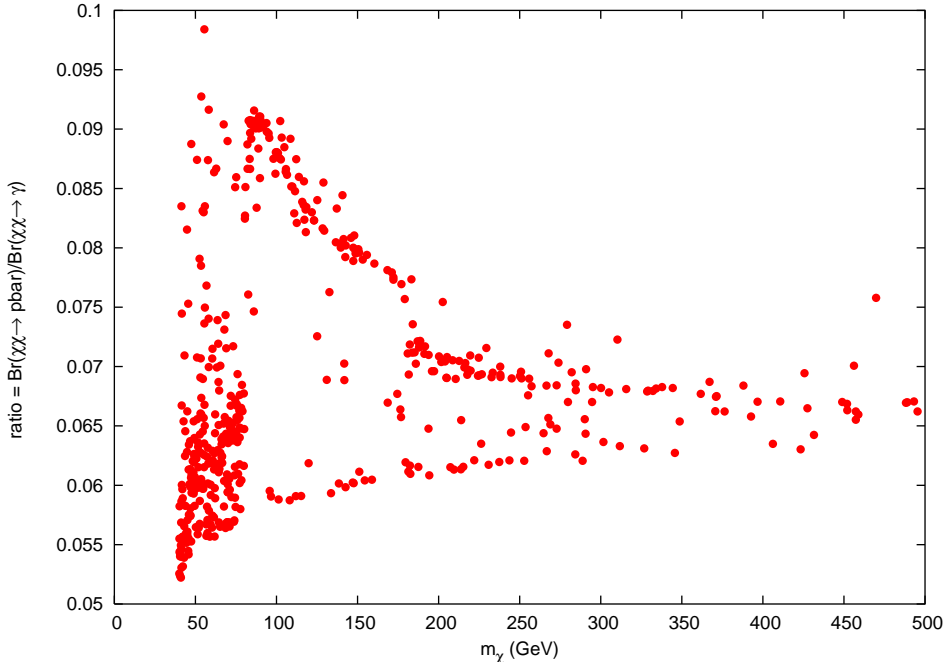


FIG. 1: $\frac{Br(\chi\chi \rightarrow \bar{p})}{Br(\chi\chi \rightarrow \gamma)}$ as a function of neutralino mass. Thresholds for \bar{p} and γ -ray kinetic energies are taken as 0.5 GeV.

conservative MSSM. A general practice in phenomenological studies is to assume some simple relations between the parameters. Following the assumptions in DarkSUSY [14] we take seven free parameters during the calculation of DM production and annihilation, i.e., the higgsino mass parameter μ , the wino mass parameter M_2 , the mass of the CP-odd Higgs boson m_A , the ratio of the Higgs Vacuum expectation values $\tan\beta$, the scalar fermion mass parameter $m_{\tilde{f}}$, the trilinear soft breaking parameter A_t and A_b . All the sfermions are taken with a common soft-breaking mass parameter $m_{\tilde{f}}$; all trilinear parameters are zero except those of the third family; the bino and wino have the mass relation, $M_1 = 5/3 \tan^2 \theta_W M_2$, coming from the unification of the gaugino mass at the grand unification scale.

A random scan in the 7-dimensional parameter space of MSSM is performed using the package DarkSUSY [14]. We assume these parameters to range as follows: $50 \text{ GeV} < |\mu|$, M_2 , M_A , $m_{\tilde{f}} < 10 \text{ TeV}$, $1.1 < \tan\beta < 61$, $-3m_{\tilde{q}} < A_t$, $A_b < 3m_{\tilde{q}}$, $\text{sign}(\mu) = \pm 1$. We find the γ -ray spectrum with $m_\chi = 40 - 50 \text{ GeV}$ (after being added to the background γ -ray spectrum) can fit the EGRET data very well, which is consistent with the result of de Boer et al. [8]. However, the branching ratio to γ rays varies by a few order of magnitude for different models, and only models with large branching ratio into γ -rays can account for the

“GeV excess”. We also calculate the branching ratio into antiprotons since the \bar{p} flux is a sensitive test of the DM model.

In Fig. 1 we give the ratio of neutralino annihilation into \bar{p} and γ -rays as a function of neutralino mass. We find $\frac{Br(\chi\chi\rightarrow\bar{p})}{Br(\chi\chi\rightarrow\gamma)} \approx \frac{1}{20} - \frac{1}{10}$ above the threshold energy $E_{th} = 0.5$ GeV for $m_\chi = 40 - 500$ GeV. For light neutralinos, the variation of the ratio in the parameter space is at most as large as a factor of 2. For heavy neutralinos the variation is very small, and the reason is that \bar{p} and γ -rays are coming from the same final states, thus they are closely related. Below, we choose $m_\chi = 48.8$ GeV to explain the EGRET data which predicts $\Omega h^2 = 0.09$ and $\frac{Br(\chi\chi\rightarrow\bar{p})}{Br(\chi\chi\rightarrow\gamma)} \approx 0.055$ for the threshold energy $E_{th} = 0.5$ GeV. Actually for m_χ between $40 \sim 50$ GeV the annihilated γ -ray spectra are almost identical. A few models also show similar branching ratio as in our chosen model (e.g., for $m_\chi = 41.13, 41.21$ GeV).

B. Astrophysics factor

The astrophysics factor determining the annihilation fluxes is defined as $\Phi^{astro} = \int_V \frac{\rho^2}{d^2} dV$ with d the distance to the source of γ -ray emission, ρ the density profile of DM, and V the volume in which annihilation taking place. In the de Boer model, the authors adopt a cored Galactic halo model with two DM rings, boosting the γ -ray flux by a factor of the order ~ 100 . In our work we take a cuspy NFW [15] (or Moore [16]) profile. Especially we take the contribution from subhalos into account to enhance the annihilation signals.

High resolution simulations of cosmological structure evolution reveal that in the cold DM scenario the structures form hierarchically and a large number of substructures survive in the galactic halos. A fraction of about 10% of the total halo mass may have survived tidal disruption and appear as distinct and self-bound substructures inside the virialized host halos. The existence of substructures will enhance the annihilation rate greatly by enhancing the astrophysics factor in Eq. (1).

The mass function and spatial function of subhalos are given by N-body simulations. A simple analytical fit to simulations allows to write the probability of a subhalo with mass m appearing at position r as [17]

$$n(m, r) = n_0 \left(\frac{m}{M_{vir}} \right)^{-1.9} \left(1 + \left(\frac{r}{r_H} \right)^2 \right)^{-1}, \quad (2)$$

where n_0 is the normalization factor so that about 10% of the halo mass is enclosed in

subhalos, $M_{vir} \approx 1.0 \times 10^{12} M_{\odot}$ is the Galactic halo mass, $r_H = 0.14 r_{vir} \approx 29$ kpc is the core radius for the distribution of subhalos. The result given above agrees well with that of another recent simulation by Gao et al. [18].

The DM density profile within each subhalo is taken as the NFW [15], Moore [16] and a cusplier form [19] as $\rho = \frac{\rho_s}{(r/r_s)^\gamma (1+r/r_s)^{3-\gamma}}$ with $\gamma = 1.7$. The last form is favored by the simulation conducted by Reed et al. [20], which gives that $\gamma = 1.4 - 0.08 \log(M/M_*)$, for the subhalo mass of $0.01 M_* \sim 1000 M_*$ with a large scattering, increasing as the subhalo mass decreases. Small halos with large $\gamma = 1.5 - 2$ are also found by Diemand et al. [21]. We take $\gamma = 1.7$ for the whole range of subhalo masses as a simple approximation.

We calculate the concentration parameter c_v by adopting the semi-analytic model of Bullock et al. [22], which describes it as a function of the viral mass and redshift. We adopt the mean $c_v - m_{sub}$ relation at redshift zero. The scale radius is then determined by $r_s^{nfw} = r_v/c_v$, $r_s^{moore} = r_s^{nfw}/0.63$ and $r_s^\gamma = r_s^{nfw}/(2 - \gamma)$ for the three density profiles respectively. Another factor determining the γ -ray flux is the core radius, r_{core} , within which the DM density should be kept constant due to the balance between the annihilation rate and the rate of DM particles falling into this region [23]. The core radius r_{core} is approximately $10^{-8} \sim 10^{-7}$ kpc for $\gamma = 1.7$ and about $10^{-9} \sim 10^{-8}$ kpc for the Moore profile.

Along a direction (θ, ϕ) , the subhalos contribute to the ‘‘astrophysical factor’’ $\Phi^{astro} = \int_{l.o.s} \Phi^{sub} dN_{sub}(\theta, \phi)$, where $\Phi^{sub} = \int_{V_{sub}} \frac{\rho^2}{d^2} 4\pi r^2 dr$ is the astrophysical factor for a single subhalo, and N_{sub} is the number density of subhalos. When we calculate the integration along the line-of-sight starting from the Sun, we get the Jacobian determinant as $\frac{r'}{r}$, with r' the distance from the subhalo to the Sun. The minimal subhalos can be as light as $10^{-6} M_{\odot}$ as shown by the recent simulation conducted by Diemand et al. [21], while the maximal mass of substructures is taken to be $0.01 M_v$ [24]. The tidal effects are taken into account based on the ‘‘tidal approximation’’ [24], where subhalos are disrupted near the Galactic center (GC). The total signal flux comes from the annihilation in the subhalos and in the smooth component.

In Fig. 2, we show the factor Φ^{astro} from the smooth component, the subhalos and the total contribution as a function of the direction to the GC. The Φ^{astro} from subhalos is almost isotropic in all directions as the Sun is near the GC compared with the viral radius r_{vir} of the Galactic halo. The largest enhancement for $\gamma = 1.7$ subhalos is observed at large angles and can reach 2 orders of magnitude. This enhancement depends on the value of

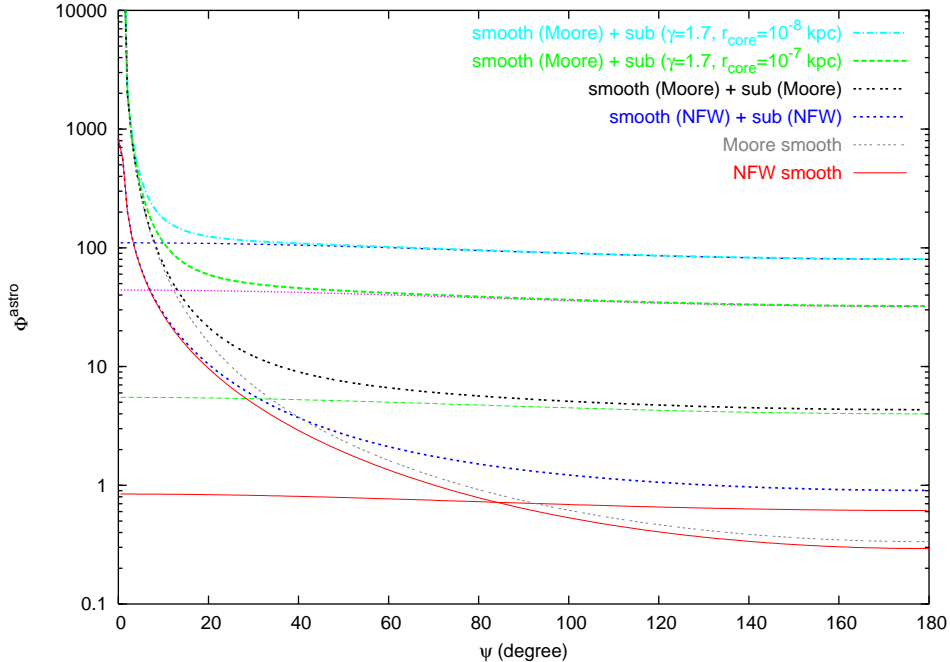


FIG. 2: The astrophysical factor Φ^{astro} (in unit of $(GeV/cm^3)^2 kpc Sr^{-1}$) from different directions. The almost horizontal lines correspond to the contributions from subhalos only.

r_{core} , while for the Moore profile the enhancement is about one order of magnitude, and for for the NFW profile only about 3 times larger. The Φ^{astro} for Moore and NFW profiles is not sensitive to r_{core} [24]. We also notice that near the GC there is no enhancement. This is actually a very important difference from the model given by de Boer where the “boost factor” is universal [8]. Given the factor Φ^{astro} and the SUSY model we can predict the γ -ray flux from neutralino annihilation.

In the next section we give the background diffuse γ -rays from CR interactions with the ISM.

III. THE CONVENTIONAL MODEL

The optimized model of Strong et al. reproduces the diffuse γ rays assuming interstellar proton and electron spectra different from those locally measured. However, the required fluctuation of the proton spectrum may be not realistic. The works of de Boer et al. have strongly indicated that DMA may account for the diffuse γ ray excess [8]. Therefore our first attempt is to build a propagation model including contribution from DMA based on

the conventional CR model assuming universal CR spectra.

We adopt the GALPROP package [5, 25] to calculate the propagation of CRs and production of Galactic background diffuse γ rays. It was shown that an explanation of the EGRET data in *all* sky directions in the conventional model is not an easy task, even including the contribution from DMA—considering that DMA provides only a single extra spectrum from neutralino annihilation. To give the best fit to the EGRET data, de Boer et al. [8] have to introduce arbitrary renormalization factors in different directions for the γ ray spectra given in the conventional model [6]. Since we are trying here to build a propagation model, we will not introduce any renormalization factors, but rather explain the γ ray data by adjusting the propagation parameters after adding the contribution from DMA.

After a lot of tests, we came to the following propagation parameters. The scale height of the propagation halo z_h takes the same value 4 kpc as that taken by Strong et al. in their conventional and optimized models [6]. The nuclei injection spectra share the same power law form in rigidity, and nuclei up to $Z = 28$ and all relevant isotopes are included. The CR injection spectra are given in Table I. We adopt the diffusive reacceleration propagation model. The spatial diffusion coefficient is given as a function of rigidity in the form

$$D(\rho) = \beta D_0 (\rho/\rho_0)^\delta, \quad (3)$$

where $\beta = v/c$, $D_0 = 5.4 \times 10^{28} \text{ cm}^2 \text{ s}^{-1}$, $\rho_0 = 4 \text{ GV}$, and $\delta = 0.34$. The Alfvén speed to describe the reacceleration process is $v_A = 34 \text{ km s}^{-1}$. These propagation parameters well describe the observed B/C ratio, the $^{10}\text{Be}/^9\text{Be}$ ratio, and the local measured proton and electron spectra, as shown in Fig. 3.

A major uncertainty in calculating the diffuse Galactic γ -ray emission is the distribution of molecular hydrogen, since the derivation of H_2 density from the CO data is problematic [38]. The CO-to- H_2 conversion factor X_{CO} from COBE/DIRBE studies given by Sodroski et al. [39] is about 2 – 5 times greater than the value given by Boselli et al. [40] in different Galactocentric radius. The later is based on the measurement of Galactic metallicity gradient and the inverse dependence of X_{CO} on metallicity [38]. The value of X_{CO} is then normalized to the γ -ray data [38]. Strong et al. have derived the X_{CO} by fitting the EGRET diffuse γ -ray data directly [41]. A constant $X_{\text{CO}} = (1.9 \pm 0.2) \times 10^{20} \text{ cm}^{-2}/(\text{K km s}^{-1})$ for $E_\gamma = 0.1 - 10 \text{ GeV}$ was given [41]. However, observations of particular local clouds yield lower values $X_{\text{CO}} = 0.9 - 1.65 \times 10^{20} \text{ cm}^{-2}/(\text{K km s}^{-1})$ [40]. Since the fit by Strong et al. to the EGRET

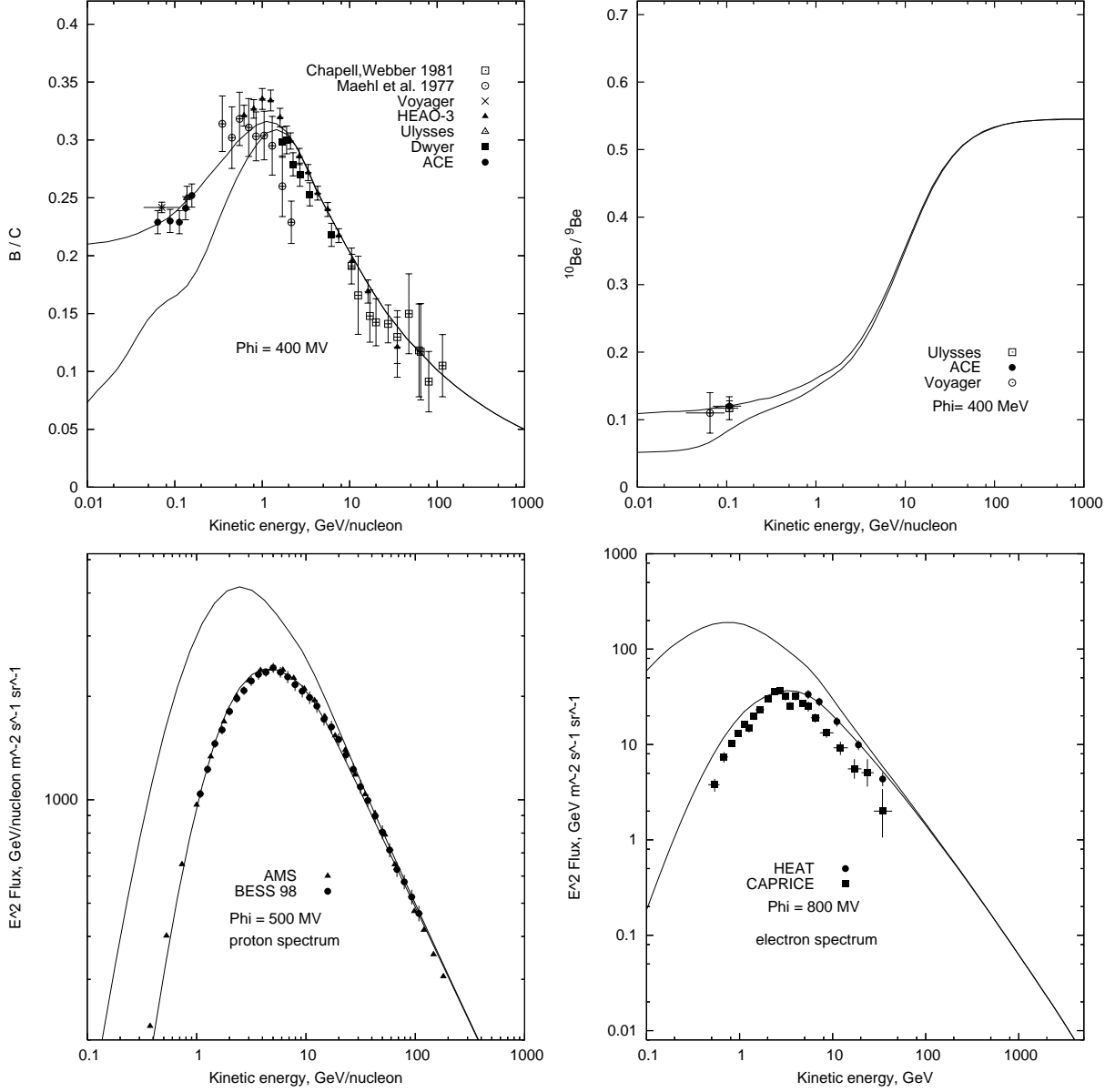


FIG. 3: Cosmic ray results in our conventional model. Lower and upper curves for B/C ratio correspond to solar modulated and local interstellar (LIS) values respectively. For $^{10}\text{Be}/^9\text{Be}$ ratio, the flat curve near 0.1 GeV/nucleon corresponds to the modulated flux and the other one is LIS. On the contrary, the lower curves for proton and electron spectra are the modulated ones and the upper are LIS. B/C data are from ACE[26], Ulysses[27], Voyager[28], HEAO-3[29] and others [30]; $^{10}\text{Be}/^9\text{Be}$ data from Ulysses[31], ACE[32] and Voyager[33]; Proton data from BESS98[34] and AMS[35]; electron data from CAPRICE[36] and HEAT[37].

TABLE I: Cosmic ray injection spectrum parameters.

	Injection index below/above break rigidity	Break rigidity GV	Normalization at E $\text{m}^{-2} \text{sr}^{-1} \text{s}^{-1} \text{GeV}^{-1}$ at GV
Nuclei Spectra ^a	1.82 / 2.36	9	4.9×10^{-2} at 100
Electron Spectrum ^a	1.60 / 2.54	4	4.86×10^{-3} at 34.5
Nuclei Spectra ^b	1.86 / 2.36	10	5×10^{-2} at 100
Electron Spectrum ^b	1.50 / 2.54	6	1×10^{-2} at 34.5

^aSpectra used in our conventional model;

^bSpectra used in our new model.

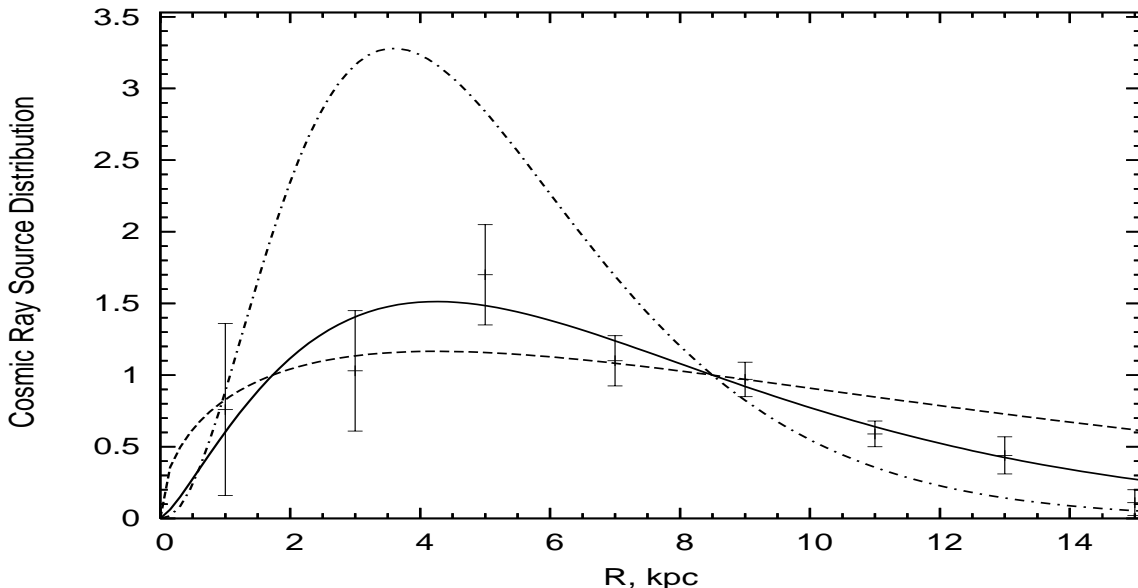


FIG. 4: Cosmic ray source distribution along the Galactocentric radius R . The source distribution is in arbitrary units. Dash-dotted line: based on pulsars[42]; dashed line: used by Strong et al.[6] and in our conventional model[13]; solid line: adopted in our new model. Vertical bars are SNR data points[43]. These distributions are normalized at $R=8.5$ kpc.

data in [41] assumes only the background contributions, we expect that it gives a larger X_{CO} than is the case with the new DMA component. We find that a smaller $X_{\text{CO}} \sim 1.0 \times 10^{20}$ molecules $\text{cm}^{-2}/(\text{K km s}^{-1})$ can give a much better description of the EGRET data below 1 GeV. After taking DMA into account, the global fitting is greatly improved. We assume for X_{CO} a constant value independent of the radius R . As shown in Ref. [38], the simple

form of X_{CO} is compensated by an appropriate form of the CR sources. We have taken the radial distribution of CR sources in the form of $(\frac{R}{R_{\odot}})^{\alpha} \exp(-\frac{\beta(R-R_{\odot})}{R_{\odot}})$, with $\alpha = 0.5$, $\beta = 1.0$, $R_{\odot} = 8.5$ kpc, and limiting the sources within $R_{\text{max}} = 15$ kpc, which are adjusted to best describe the diffuse γ -ray spectrum. The source distribution is shown in Fig. 4 (dashed line).

Following Strong et al. [6], we divide the whole sky into six regions: region A corresponds to the “inner radian”, region B is the Galactic plane excluding the inner radian, region C is the “outer Galaxy”, regions D and E cover higher latitudes at all longitudes, and region F describes the “Galactic poles”. The calculated diffuse γ spectra in the six different sky regions are given in Fig. 5. The diffuse γ ray background includes contributions from π^0 decays produced by nuclei collisions, IC scattering off the interstellar radiation field (ISRF), bremsstrahlung by electrons, and the isotropic extragalactic γ ray background (EGRB). For the regions A, B, C and D, i.e. the Galactic plane and the intermediate latitude regions, the π^0 decay contribution is dominant. At high latitude regions E and F the EGRB becomes more important. To account for the GeV excess the peak of the DMA γ ray spectrum has to have similar magnitude as the background. After adding the diffuse γ ray emission from DMA to the Galactic background, we obtain a perfect agreement with EGRET measurements for all sky directions.

The result in Fig. 5 is really a success, considering that we simply add the two kinds of diffuse γ ray contributions together, without introducing any arbitrary normalization for the background γ rays or “boost factors” for the DMA contribution. It should be noted that including the enhancement by subhalos does not exclude the ring-like structures proposed by de Boer [8, 10]. That is natural since taking the subhalos into account only enhances the signals coming from the smooth component, but does not mimic the ring-like structure, which can fit the EGRET data at different directions [8].

A. Flux of \bar{p}

We have seen in Fig. 1 that the branching ratios to γ rays and to \bar{p} are closely related. Therefore the \bar{p} flux is a sensitive test of the DMA scenario to solve the “GeV excess” problem. In [12], Bergström et al. have claimed that the de Boer model has been ruled out due to the overproduction of \bar{p} flux. In their work they adopted a simple propagation model similar to that adopted in DarkSUSY [14]. We now check the \bar{p} flux in our propagation

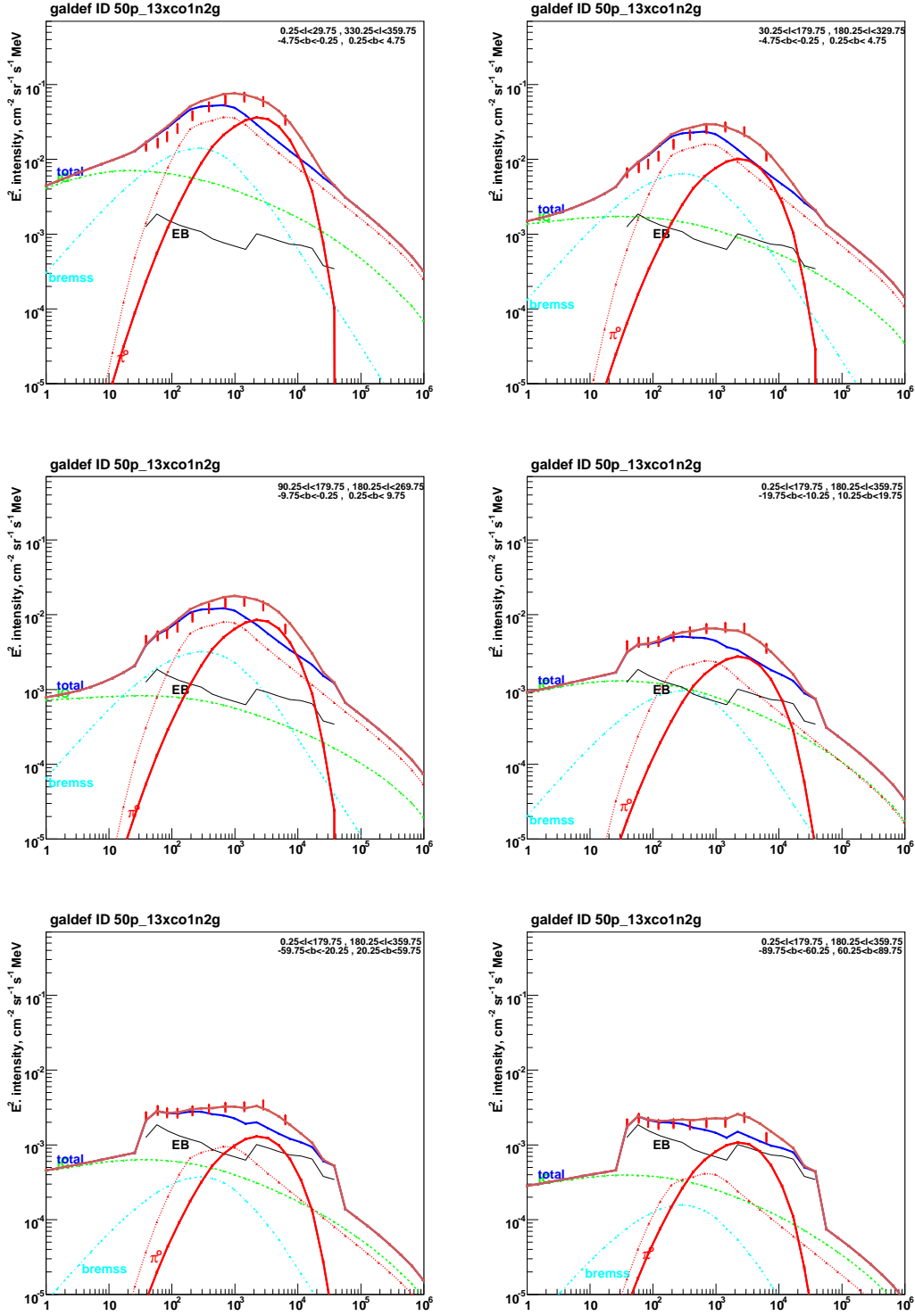


FIG. 5: Spectra of diffuse γ -rays for different sky regions (top row, regions A, B, middle C, D, bottom E, F). The model components are π^0 decay, inverse Compton, bremsstrahlung, EGRB and DMA (dark red curve).

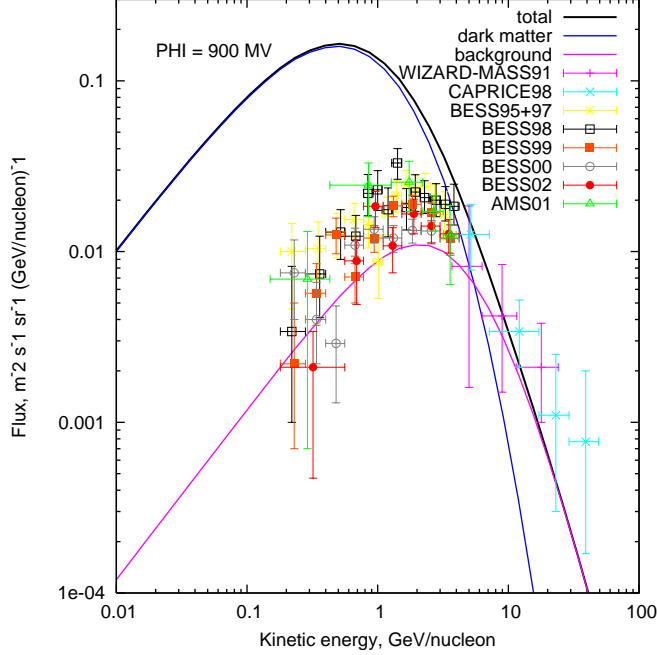


FIG. 6: Solar modulated flux of antiprotons in the conventional model. The upper/black curve represents the total \bar{p} flux. For the two lower curves, the one dominating at energies below several GeV is the DMA contribution and the other dominating at energies above several GeV stands for the contribution from CR interactions. \bar{p} data are from WIZARD-MASS91[44], CAPRICE98[45], BESS95+97[46], BESS98[47], BESS99[48], BESS00[48], BESS02[49], AMS01[50].

model.

We first calculate the source term of \bar{p} produced by neutralino annihilation adopting the same SUSY model used for the diffuse γ ray data,

$$\Phi_{\bar{p}}(r, E) = \frac{\langle \sigma v \rangle \phi(E)}{2m_{\chi}^2} \langle \rho(r)^2 \rangle, \quad (4)$$

where $\phi(E)$ is the differential \bar{p} flux at energy E due to a single annihilation, and

$$\langle \rho(r)^2 \rangle = \rho_{smooth}^2 + \langle \rho_{sub}^2 \rangle, \quad (5)$$

are contributions from the smooth DM component and subhalos. The contribution from subhalos is given by

$$\langle \rho(r)_{sub}^2 \rangle = \int_{m_{min}}^{m_{max}} n(m, r) \left(\int \rho^2 dV \right) dm, \quad (6)$$

where $n(m, r)$ is the number density of subhalos with mass m at radius r , and $\int \rho^2 dV$ is

the astrophysical factor for a single subhalo with mass m . All subhalo parameters are taken identical to those used to account for the diffuse γ rays.

We then calculate, in the same propagation model, the \bar{p} spectrum at Earth by incorporating the source term of Eq. (4) in GALPROP. Fig. 6 shows the background, the signal and the total \bar{p} fluxes. The background antiproton flux is lower than the data; this has been discussed in [6, 51]. This is another hint at the necessity of an exotic signal besides the ordinary CR secondaries. The \bar{p} flux in our model is about one order of magnitude greater than the measured data at energies lower than 1 GeV. However, we notice that our prediction is a few times lower than that by Bergström et al. [12], when they adopted the median set of propagation parameters, which are similar to the propagation parameters in our conventional model. The difference may be due to two reasons: first we adopt a different propagation model; second—and maybe more important—, we do not adopt a universal “boost factor” for the diffuse γ rays from DMA as de Boer and Bergström et al. did. The enhancement by subhalos tends to boost the γ ray and \bar{p} fluxes at large radii, as shown in Fig. 2. Therefore subhalos boost γ rays more than \bar{p} since only these \bar{p} produced within the Galactic diffusion region contribute to the \bar{p} flux on Earth.

However, these effects are not enough to give a \bar{p} flux consistent with the data. This is related to the presence of two DM rings near the solar system, that enhance the antiproton flux greatly as they are strong \bar{p} sources. We have to resort to a new propagation model to suppress the \bar{p} further and give a consistent description of all data.

IV. A NEW PROPAGATION MODEL

Inheriting the advantages of our conventional model in the last section, a new propagation model is intended to be built to account for the Galactic diffuse γ rays, and at the same time the \bar{p} flux. Degeneracies exist between the propagation parameters, mainly between the diffusion coefficient $D(\rho)$ and the height of the diffusion region z_h . Different sets of parameters can all explain the CR data but lead to very different signals from DMA [52]. If we adopt smaller z_h we can adjust $D(\rho)$ at the same time to give similar prediction of the CR data. However adopting smaller z_h leads to smaller \bar{p} flux from DMA since only \bar{p} sources within the diffusion region contribute to the flux on the Earth. The degeneracy leads to about one order of magnitude uncertainties of the \bar{p} flux when adopting different

sets of propagation parameters in Bergström et al. [12]. Therefore it is straightforward to consider a smaller height of the diffusion region to suppress the DMA signal.

The diffusion halo height is determined by fitting the CR data. It is found that the average gas density CRs crossed during their travel to the Earth is about 0.2 atoms/cm^3 , which is significantly lower than the average gas density in disk of about 1 atom/cm^3 . This is explained by the possibility that CRs are confined in a larger diffusion region than the gaseous disk, spending a longer time outside the gaseous disk. The height of the halo represents the volume of this diffusion region. In [53], Strong and Moskalenko derived $z_h = 3 - 7 \text{ kpc}$ for the four types of radioactive nuclei isotopes of $^{54}\text{Mn}/\text{Mn}$, $^{36}\text{Cl}/\text{Cl}$, $^{26}\text{Al}/^{27}\text{Al}$ and $^{10}\text{Be}/^9\text{Be}$, while the data of $^{10}\text{Be}/^9\text{Be}$ favored a smaller halo of $1.5 - 6 \text{ kpc}$. Maurin et al. found that several settings of propagation parameters with halo height z_h ranging from 1 kpc to 15 kpc could well fit the observational B/C ratio data [54, 55]. Certainly the diffusion halo height should be at least as large as the scale height of the ionized component of the interstellar gas, $\sim 700 \text{ pc}$ [56]. The halo height is also constrained by the diffuse γ ray emission at the intermediate latitude, since too small halo height will lead to too low γ ray flux at these latitudes.

Since the gas is not smoothly distributed in the disk, CRs may travel in low density regions in the disk and may not diffuse to so large a region as usually considered. As shown in [57], the gas density and the strength of magnetic fields are higher than average within molecular clouds: the molecular clouds can act as magnetic mirrors to reflect and confine the charged CR particles. In this scenario CRs may travel in a low gas density region rather than in a region with the average density. Nevertheless, the effect of molecular cloud reflection is hard to quantify. We assume the gas density that CRs crossed is lowered compared with the average gas density in the disk by a constant factor, which should be of the order of 1 since the conventional diffusion model has been very successful in describing the CR transportation. We find that a reduction factor ~ 1.5 and $z_h = 1.5 \text{ kpc}$ can reproduce all the data very well, which will be shown below. It should be noted that the reduction of the gas density crossed by CRs is the key point of this propagation model.

Taking this smaller halo height, we then adjust the diffusion coefficient and the Alfvén speed, so that we can reproduce the secondary to primary ratios, e.g. the B/C ratio. In the present model, parameters in Eq. (3) are taken as $D_0 = 1.3 \times 10^{28} \text{ cm}^2 \text{ s}^{-1}$, $\rho_0 = 4\text{GV}$ and $\delta = 0.34$. The Alfvén speed v_A is taken as 19 km s^{-1} . The injection spectra of nuclei and

electrons are given in Table I.

The CR source distribution adopted in this model is shown in Fig. 4, together with the source distribution adopted in [38], which is the same as the pulsar distribution [42], and that adopted in [5, 6], which is obtained by fitting the EGRET data with a constant X_{CO} value. The vertical bars are SNR data points from [43]. The flat source distribution derived by fitting the EGRET diffuse γ ray data is not in agreement with the distribution of SNRs [38]. As for the pulsar distribution, it is so peaked that it would aggravate the problem of reproducing the relatively smooth EGRET flux profile along the Galactic Plane [58]. In addition, the pulsar distribution is probably not sufficiently reliable to trace the SNRs accurately. In fact, only a proportion of about one in ~ 100 known pulsars appears to be convincingly associated directly with SNRs [59]. It is very interesting that in our new model, the source distribution consistent with SNRs data (solid line in Fig. 4) can give a better description of the diffuse γ ray data with a constant CO-to-H₂ conversion factor $X_{\text{CO}} \sim 1.0 \times 10^{20}$ molecules $\text{cm}^{-2}/(\text{K km s}^{-1})$ than the other two distribution functions. The radial source distribution has the same form as the previous one with $\alpha = 1.35$, $\beta = 2.7$.

In Fig. 7, we show the results of B/C, $^{10}\text{Be}/^9\text{Be}$, spectra of protons and electrons as predicted by this new propagation model. The stable secondary to primary ratio B/C and the unstable to stable secondaries $^{10}\text{Be}/^9\text{Be}$ show that our model reproduces the experimental data very well. In this model the interstellar proton spectrum is taken to be the locally observed spectrum since the energy loss of proton is negligible. The interstellar electron spectrum has an intensity normalization at high energies different from the local one, similar to the electron spectrum adopted by Strong et al. in [6] but with smaller fluctuations. We will show below that this model can also reproduce the diffuse γ ray and \bar{p} data well.

A. Diffuse γ -rays and \bar{p} flux

In order to give γ ray and \bar{p} fluxes consistent with experimental data, we also changed the DM ring parameters slightly: the inner ring is now located at $R = 3.5$ kpc and the outer ring is moved from $R = 14$ kpc to 16 kpc. On one hand, the position of rings are not crucial parameters to fit the EGRET data: indeed, a slight change will not vary the prediction of diffuse γ rays much. On the other hand, the rings are mainly helpful to explain the diffuse γ rays at intermediate latitudes; there are not enough to account for the GeV excess elsewhere,

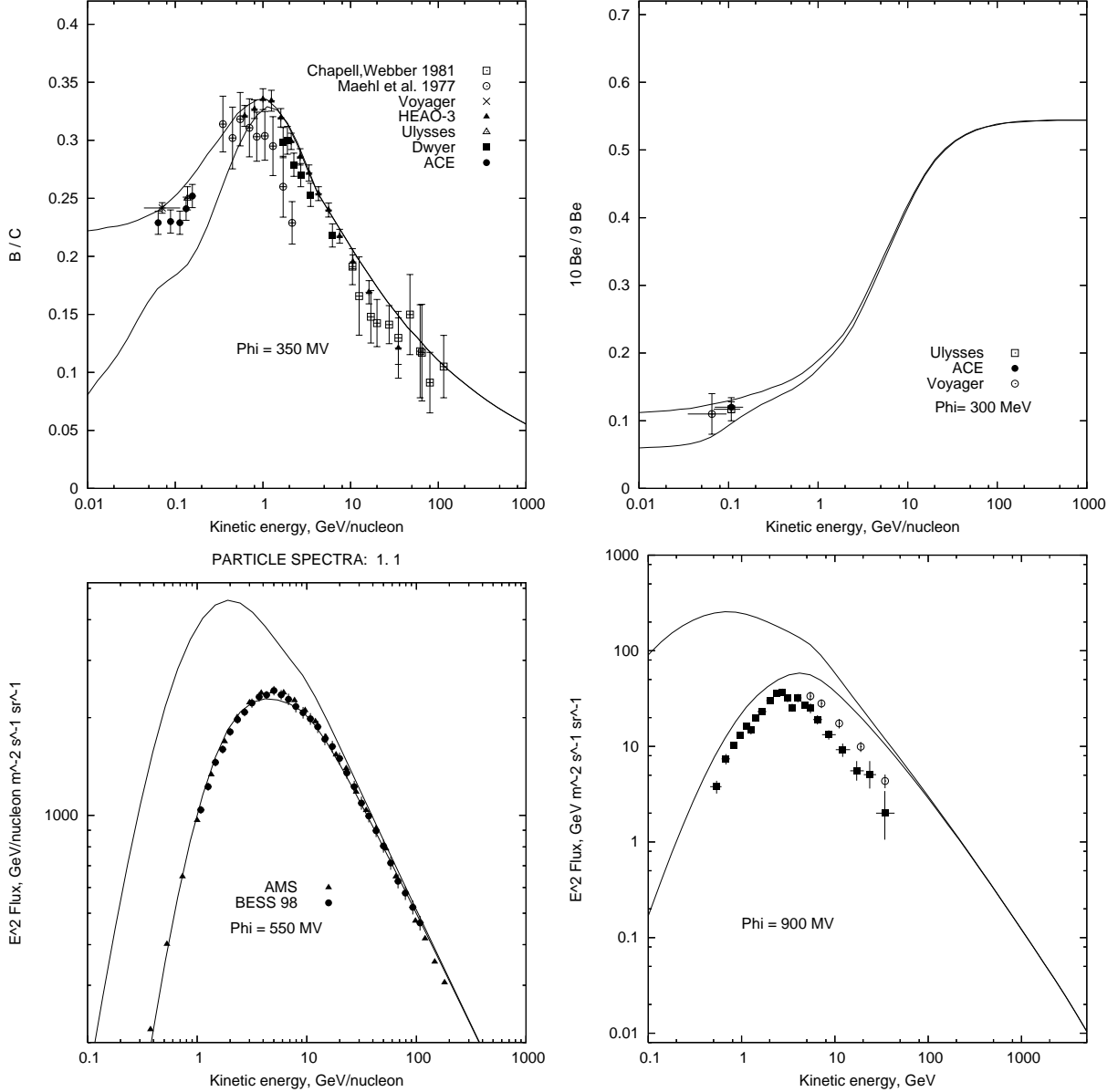


FIG. 7: The CR spectra in our new model. Curves and data are the same as in Fig. 3.

such as in regions D and E (if only the smooth DM component is included). However, our consideration of subhalos helps to enhance γ ray emissions at large radii as shown in Fig. 2. Therefore, we do not need so large γ ray emissions from the two rings to contribute to the intermediate latitudes as done in the de Boer model, and we can move them slightly far away from the solar system. It is interesting to note that the analysis of the HI gas flaring by Kalberla et al. also favored a DM ring located at a large radius of ~ 17.5 kpc [60].

We have checked that these soft modulation of ring parameters did not change the rotation

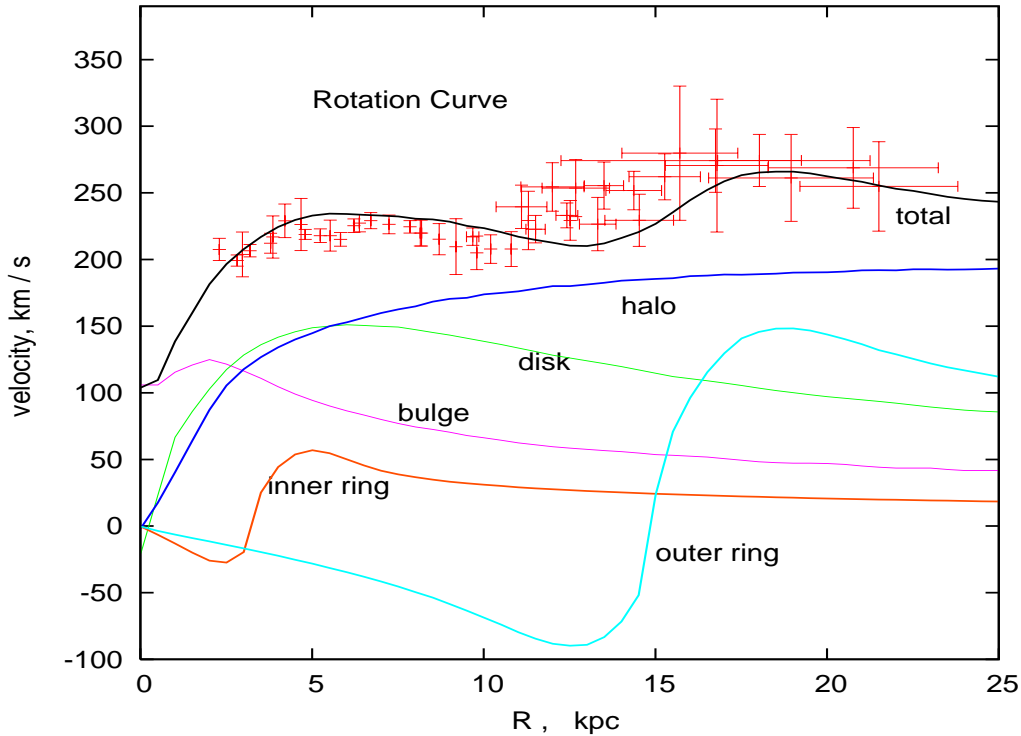


FIG. 8: The rotation curve in our new propagation model.

curve significantly. Fig. 8 shows the rotation curve for the present model. The contributions from the DM smooth halo, the two DM rings, and the bulge and disk are included. It can be seen that the rotation curve is consistent with data.

Adding the background diffuse γ rays from CRs and those from DMA *directly*, we find the calculated diffuse γ rays are well consistent with observations. The diffuse γ ray spectra in the six sky regions are shown in Fig. 9. The prediction in the new propagation model is in good agreement with EGRET data.

Figs. 10, 11 and 12 display the diffuse γ longitudinal and latitudinal profiles in our present model. The line styles in these figures are the same as those given in Figs. 5 and 9, representing contributions from π^0 decay, IC, bremsstrahlung and EGRB respectively. The solid red line is the total contribution from the background γ rays (solid blue) and DMA signals. From these figures, it is obvious that the DMA component is essential to explain the profiles above 500 ~ 1000 MeV. We notice that the longitudinal profiles at low latitude ($|b| < 5^\circ$) and the latitudinal profiles in the outer Galaxy with $30^\circ < l < 330^\circ$ are in fairly good agreement with the EGRET data. However, for the latitudinal profiles in the inner Galaxy ($330^\circ < l < 30^\circ$), we also find that the intensities at intermediate latitudes

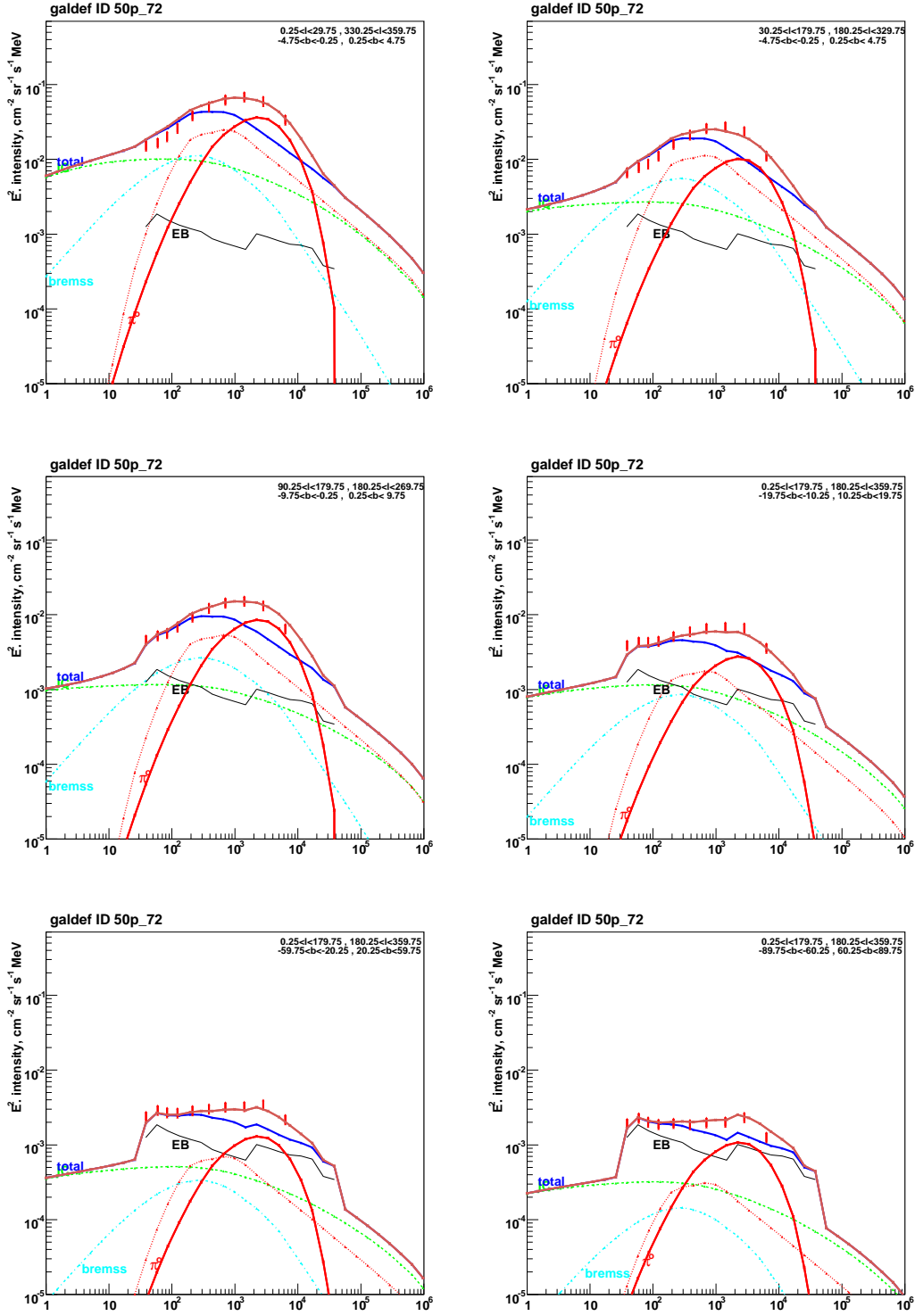


FIG. 9: Diffuse gamma ray spectra in the six sky regions predicted by the new propagation model (top row, regions A, B, middle C, D, bottom E, F). The various contributions are π^0 decay, inverse Compton, bremsstrahlung, EGRB and DMA (dark red curve).

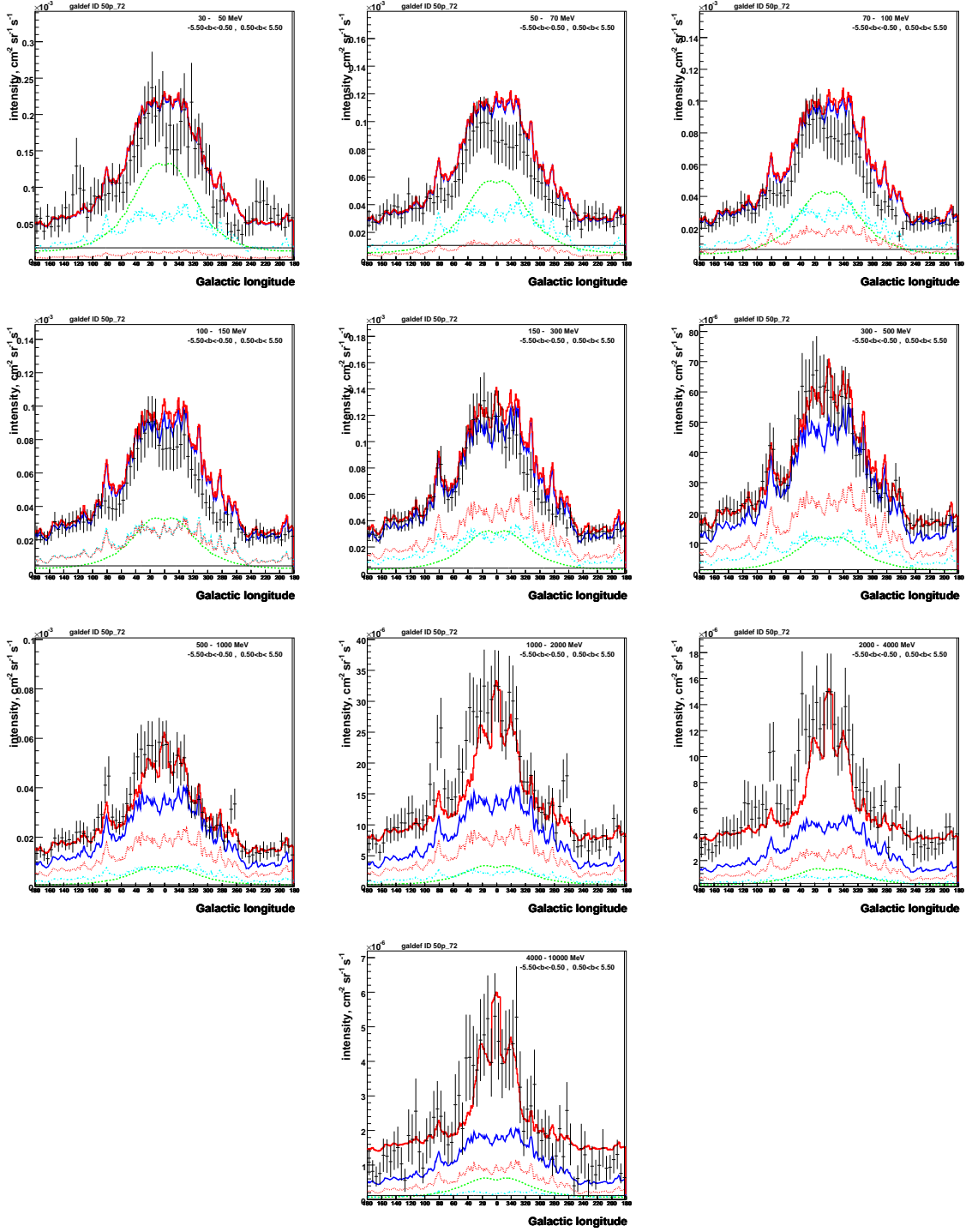


FIG. 10: Longitude profiles at low latitudes ($|b| < 5.5$) in the new propagation model, compared with EGRET data in 10 energy ranges from 30 MeV to 10GeV.

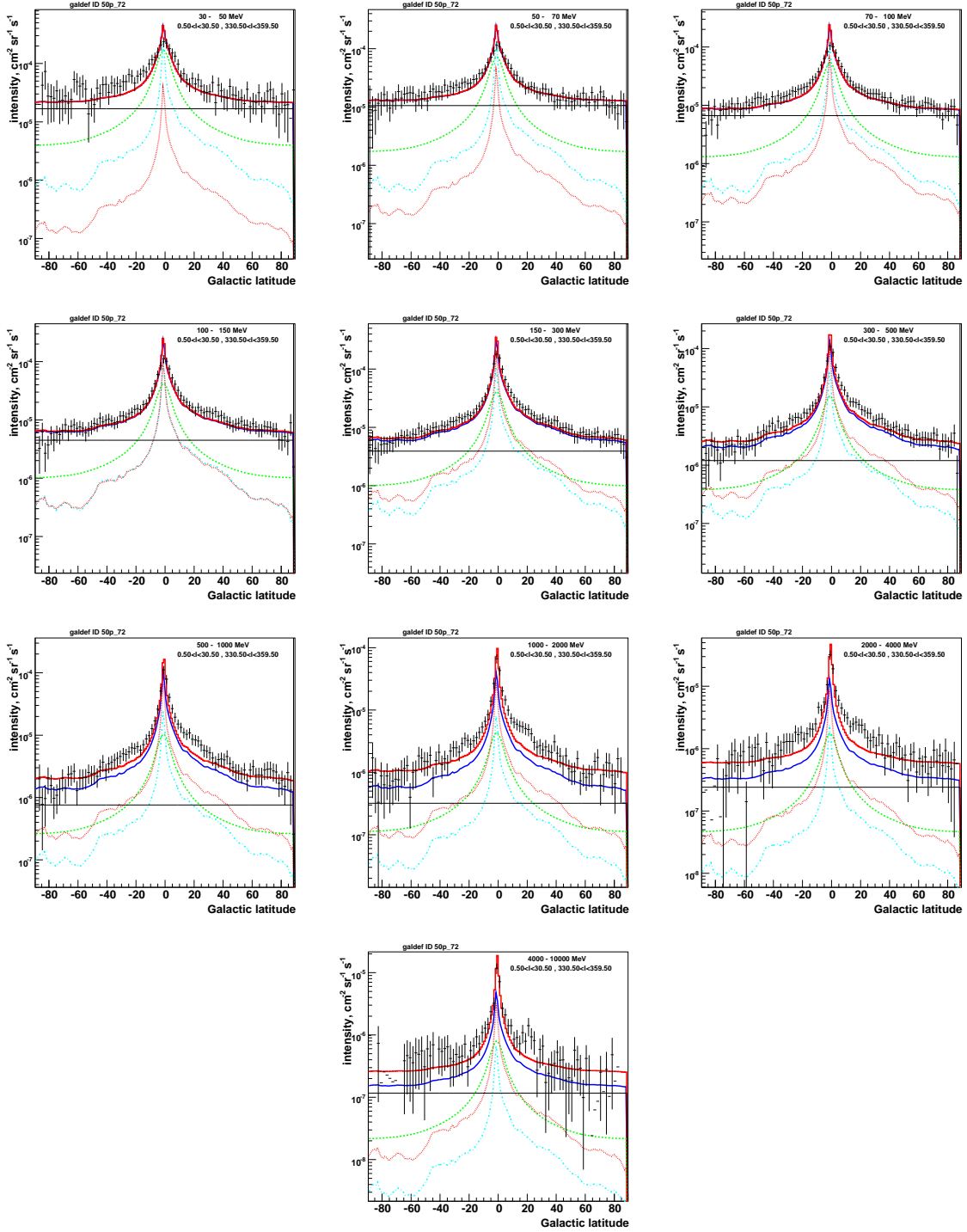


FIG. 11: Latitude profiles in the inner Galaxy $|l| < 30^\circ$ in the new propagation model, compared with EGRET data in 10 energy ranges from 30 MeV to 10GeV.

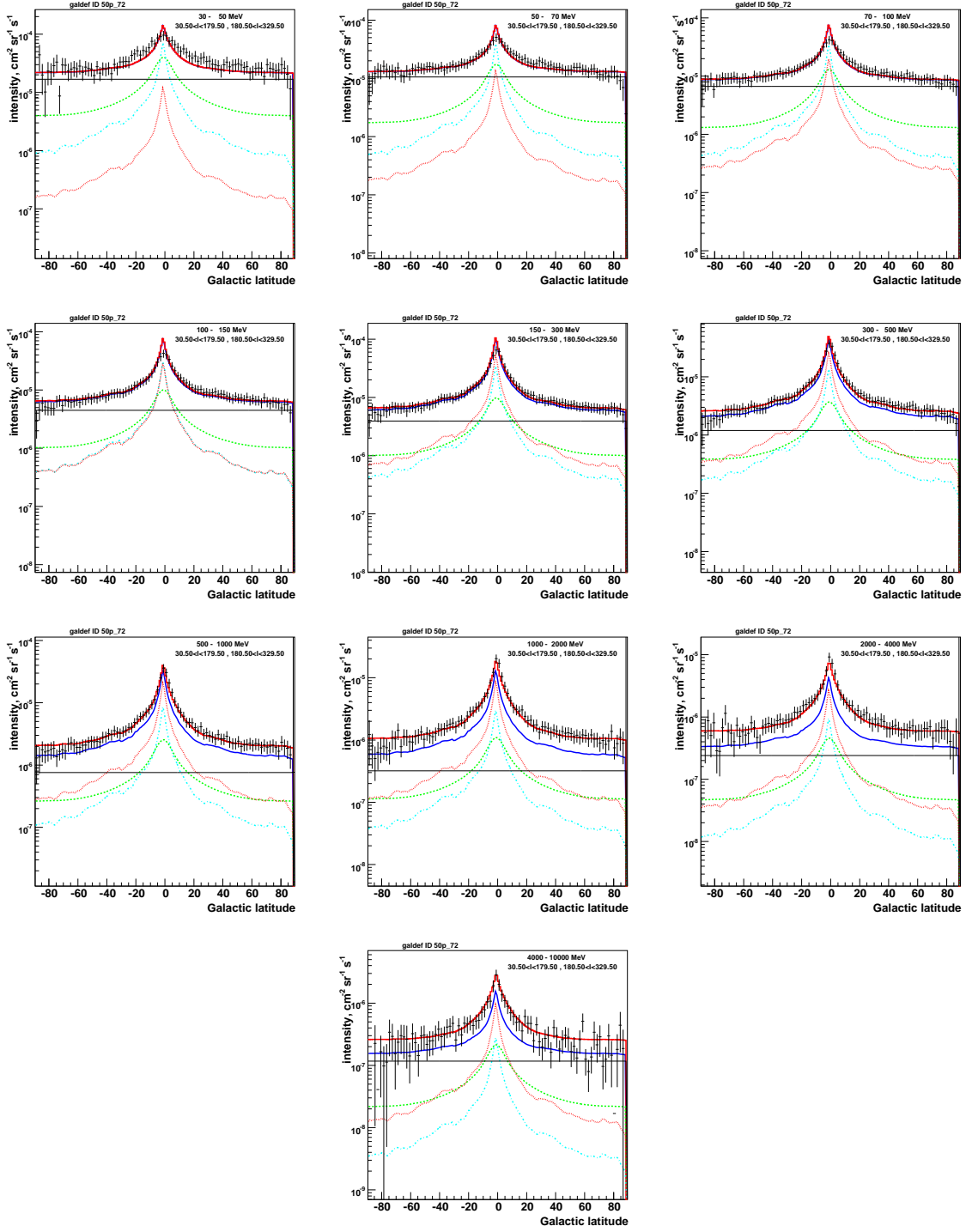


FIG. 12: Latitude profiles in the longitude ranges $30^\circ < l < 330^\circ$ in the new propagation model, compared with EGRET data in 10 energy ranges from 30 MeV to 10GeV.

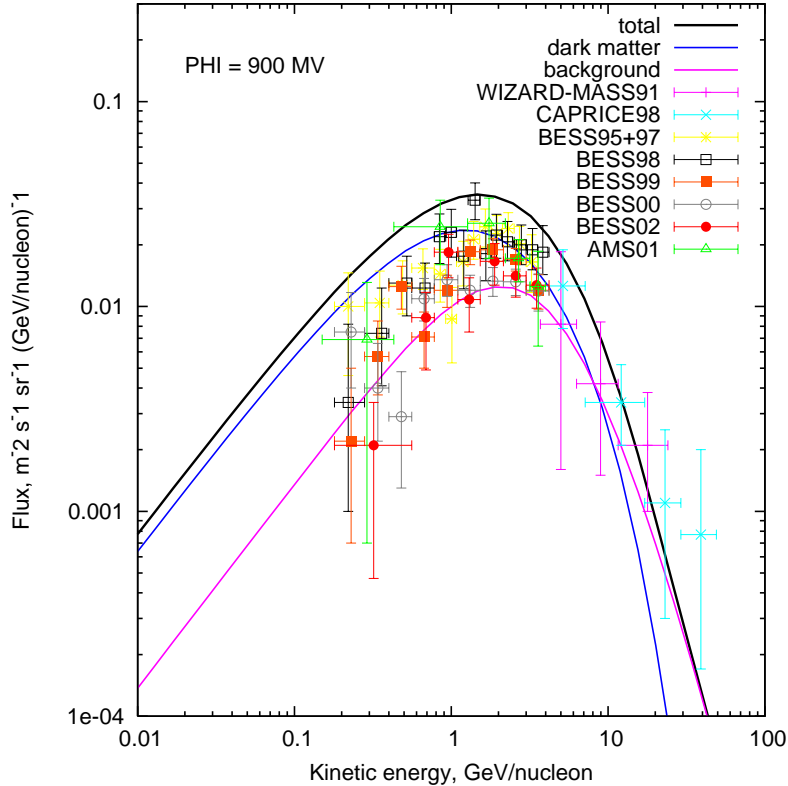


FIG. 13: Flux of antiprotons after solar modulation in the new propagation model. Lines and data are the same as in Fig. 6.

$10^\circ \lesssim b \lesssim 30^\circ$ are lower than measurements at energies from 500 MeV to 4000 MeV. A similar excess is present in the “optimized model” [6], in which it is pointed out that this may be related to an underestimate of the ISRF in the Galactic halo and that a factor of ~ 2 uncertainty on the ISRF is quite possible due to the complexity of its calculation [6]. Furthermore, the smaller z_h adopted here shallows the distribution of electrons, which may also contribute to this discrepancy.

Finally, the antiproton flux is given in Fig. 13. Below ~ 8 GeV, the \bar{p} flux from DMA dominates the CR secondary \bar{p} . The total \bar{p} flux is a bit higher than the best fit value of the experimental data ². However due to large errors of the present experimental data, the prediction is still consistent with data within 1σ . Forthcoming high precision \bar{p} measurements

² Here we take the solar modulation potential $\Phi = 900$ MV. In fact, the modulation parameter is not a free parameter for different CR species, but depends on the solar activities. The measurements of the \bar{p} flux were taken from the solar maximum (BESS00, BESS02) to the solar minimum (BESS95).

by PAMELA [61] and AMS02 [62] will be helpful to determine if the present model is viable. It should be noted that our model has the potential to further suppress the \bar{p} flux, by changing the rings position and the diffusion height z_h .

In [63], de Boer et al. introduced an anisotropic propagation model to greatly suppress the \bar{p} flux. In their model, only the \bar{p} from DMA within the gaseous disk is confined by magnetic field and contributes to the \bar{p} flux at Earth. The \bar{p} from DMA above the gaseous disk is blown away and has no contribution to the local \bar{p} flux. In order to reproduce the B/C data, they introduced a grammage parameter $c = 12$ so that the secondaries and the resident time are increased by this factor, as a result of the molecular clouds confinement of charged particles. However, we think it may be hard to reproduce the diffuse γ ray data at intermediate and high latitudes in this model, since the CRs above the gas disk are quickly blown away and produce very low γ ray emissivity. Our model gives consistent Galactic diffuse γ rays and \bar{p} flux with experimental data simultaneously without drastic modifications of the GALPROP model.

V. SUMMARY AND DISCUSSION

In this work we propose to solve the “GeV excess” problem of the Galactic diffuse γ rays by developing a new propagation model which includes contributions from DMA. We have shown that this propagation model can well reproduce the B/C, $^{10}\text{Be}/^9\text{Be}$ data and spectra of protons and electrons. The Galactic diffuse γ ray spectrum at different sky regions and its profile as a function of longitude and latitude are also shown to describe the EGRET data very well, if the DMA contribution is included. The \bar{p} flux in this model is consistent with experimental data within 1σ . Compared with previous works [6, 8], our model does not introduce a normalization of the interstellar proton intensity different from the local one (as it should be universal due to the negligible energy loss of protons). Furthermore, neither the “boost factors” to the DMA signals nor the arbitrary renormalization of the Galactic γ -ray background are needed in our model to explain the EGRET data.

In our model, the \bar{p} flux from DMA is suppressed by the following changes compared with the de Boer model [8]: 1) the smaller z_h helps to suppress the \bar{p} flux from the smooth component of DM. The average gas density CRs crossed may be smaller than the average gas density in the disk, as shown in [57]. This fact tends to favor a smaller height of the CR

diffusion region. 2) We do not adopt a universal “boost factor” for γ rays and \bar{p} . Since the enhancement by subhalos is larger at large radii, the boost of \bar{p} at the solar neighborhood is smaller than the boost of γ rays. 3) The ring parameters are slightly adjusted, which does not change the γ ray profile while greatly suppressing the \bar{p} flux. This is because the distance dependence of the \bar{p} propagation is steeper (exponential decrease) than r^{-2} of γ -rays [64].

A potential problem of this model is related to the \bar{p} flux, which is consistent with data, but cannot best fit the data. Adjusting the propagation or DM parameters (such as the rings) can further lower the \bar{p} flux. However, more fine-tuning is required to fit the γ -ray and rotation curve data. Note a new explanation of the “GeV excess” was given as an instrumental biases contaminating the EGRET data [65]. However, whether this conjecture is correct or not cannot be confirmed at the moment. Forthcoming precise observations, such as GLAST [66], PAMELA [61] and AMS02 [62], will be decisive to validate or disprove this model. At present, because of the fundamental importance of the DM problem, we think that any possible implication of DM signals deserves a serious treatment.

Acknowledgments

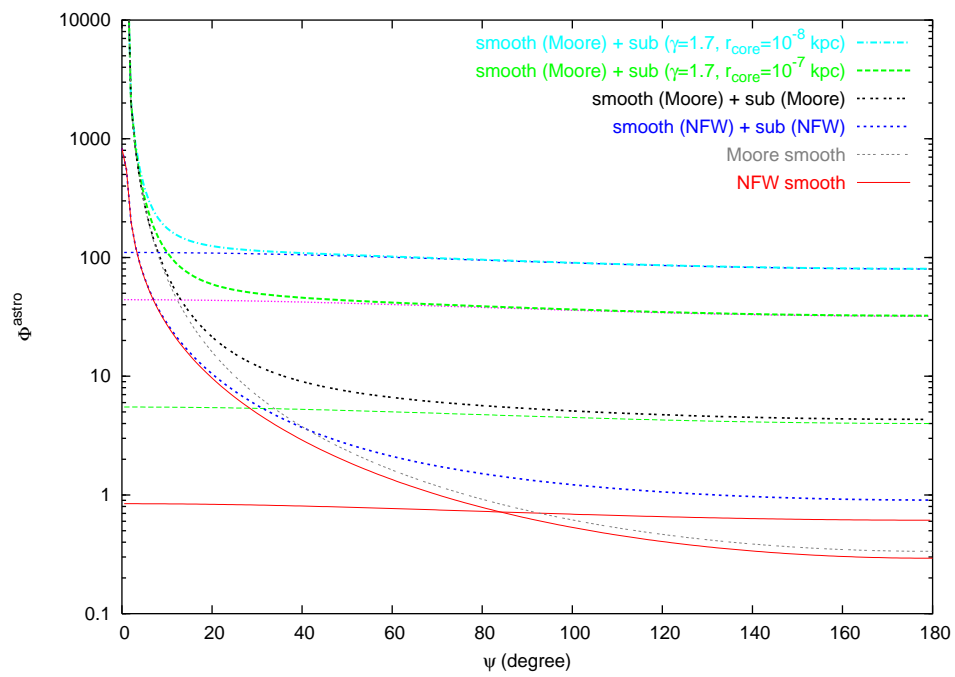
We thank the anonymous referee for helpful comments on the manuscript and D. Maurin and J. Lavalle for improvement on English. This work is supported by the NSF of China under the grant Nos. 10575111, 10773011 and supported in part by the Chinese Academy of Sciences under the grant No. KJCX3-SYW-N2.

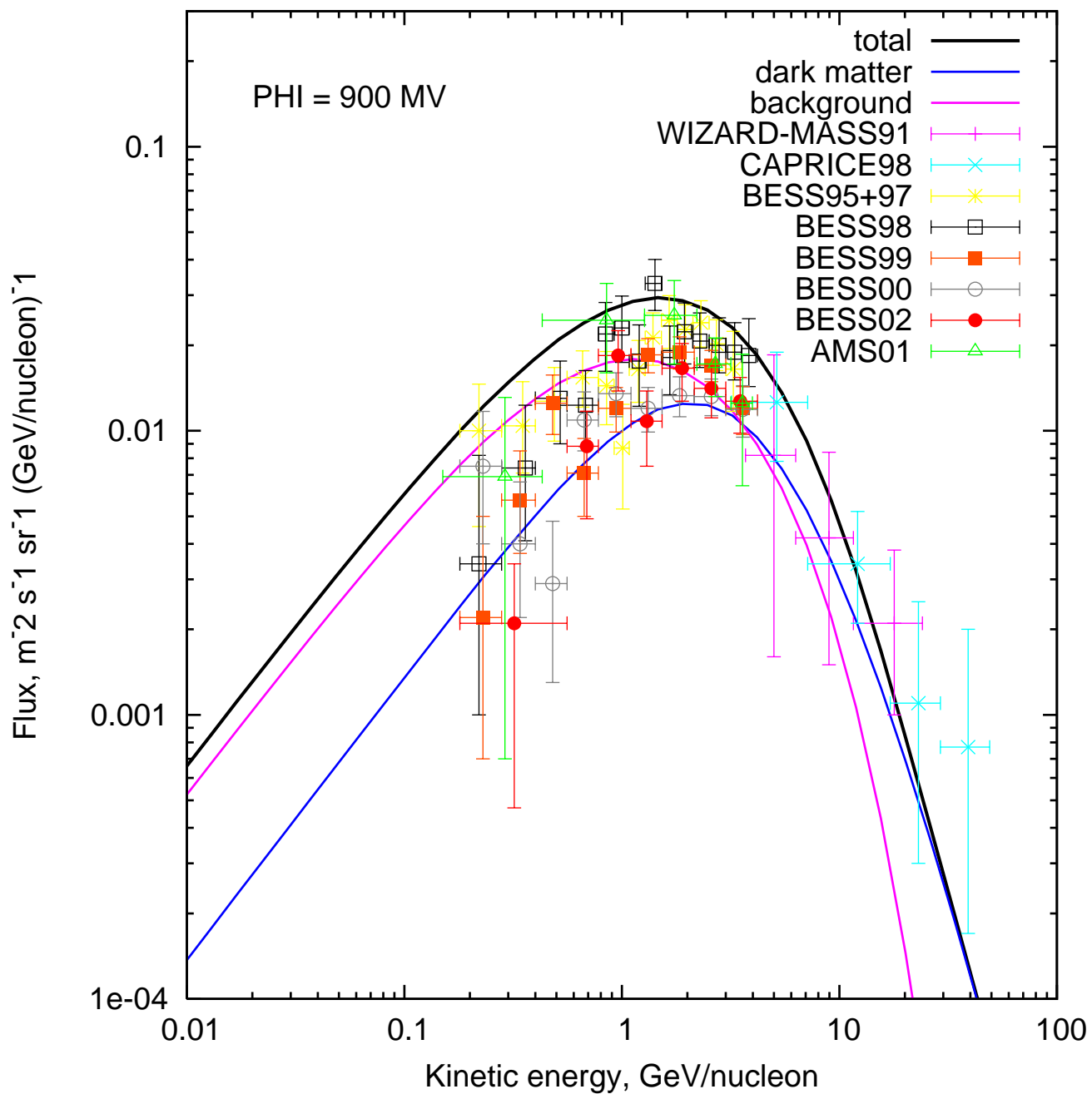
-
- [1] J. L. Zhang, X. J. Bi, H. B. Hu, *Astron. & Astrophysics* **449**, 641 (2006); I. V. Moskalenko, T. A. Porter, A.W. Strong, *Astrophys. J.* **640**, L155 (2006).
 - [2] P. Sreekumar, *Suppl. to J. Astrophys. Astr.* **16**, 285 (1995); D. A. Kniffen *et. al.*, *Astron. & Astrophys. Suppl. Ser.* **120**, 615 (1996).
 - [3] S. D. Hunter *et. al.*, *Astrophys. J.* **481**, 205 (1997).
 - [4] P. Gralewicz, J. Wdowczyk, A. W. Wolfendale, L. Zhang, *Astron. & Astrophysics* **318**, 925 (1997); M. Mori, *Astrophys. J.* **478**, 225 (1997); T. A. Porter, R. J. Protheroe, *J. Phys. G*

- 23**, 1765 (1997); M. Pohl, J. A. Esposito, *Astrophys. J.* **507**, 327 (1998); F. A. Aharonian, A. M. Atoyan, *Astron. & Astrophysics* **362**, 937 (2000).
- [5] A. W. Strong, I. V. Moskalenko, O. Reimer, *Astrophys. J.* **537**, 763 (2000).
- [6] A. W. Strong, I. V. Moskalenko, O. Reimer, *Astrophys. J.* **613**, 962 (2004).
- [7] E. G. Berezhko, H. J. Völk, *Astrophys. J.* **540**, 923 (2000).
- [8] W. de Boer, C. Sander, A. V. Gladyshev and D. I. Kazakov, *Astron. & Astrophysics* **444**, 51 (2005).
- [9] W. de Boer, C. Sander, V. Zhukov, A. V. Gladyshev and D. I. Kazakov, *Phys. Lett. B* **636**, 13 (2006);
- [10] W. de Boer, I. Gebauer, M. Weber, C. Sander, V. Zhukov, D. Kazakov, arXiv:0710.5106; W. de Boer, arXiv:0711.1912.
- [11] A. W. Strong, I. V. Moskalenko, *Proc. 27th Int. Cosmic Ray Conf. (Hamburg)*, pp.1964-1967.
- [12] L. Bergstrom, J. Edsjo, M. Gustafsson, P. Salati, *JCAP* 0605, 006 (2006).
- [13] X. J. Bi, J. Zhang, Q. Yuan, J. L. Zhang, H. S. Zhao, astro-ph/0611783.
- [14] P. Gondolo, J. Edsjo, P. Ullio, L. Bergstrom, M. Schelke, E.A. Baltz, *JCAP* 0407, 008 (2004).
- [15] J. F. Navarro, C. S. Frenk S. D. M. White, *Mon. Not. R. Astron. Soc.* **275**, 56 (1995); J. F. Navarro, C. S. Frenk S. D. M. White, *Astrophys. J.* **462**, 563 (1996); J. F. Navarro, C. S. Frenk S. D. M. White, *Astrophys. J.* **490**, 493 (1997).
- [16] B. Moore, F. Governato, T. Quinn, J. Stadel, & G. Lake, *Astrophys. J.* **499**, 5 (1998); B. Moore, T. Quinn, F. Governato, J. Stadel, & G. Lake, *Mon. Not. R. Astron. Soc.* **310**, 1147 (1999).
- [17] J. Diemand, B. Moore, J. Stadel, *Mon. Not. R. Astron. Soc.* **352**, 535 (2004);
- [18] L. Gao, S.D.M. White, A. Jenkins, F. Stoehr, V. Springel, *Mon. Not. R. Astron. Soc.* **355**, 819 (2004).
- [19] S. H. Zhao, *Mon. Not. R. Astron. Soc.* **278**, 488 (1996).
- [20] D. Reed, F. Governato, L. Verde, J. Gardner, T. Quinn, J. Stadel, D. Merritt, G. Lake, *Mon. Not. R. Astron. Soc.* **357**, 82 (2005).
- [21] J. Diemand, B. Moore, J. Stadel, *Nature* **433**, 389 (2005); J. Diemand, M. Kuhlen, P. Madau, *Astrophys. J.* **649**, 1 (2006).
- [22] J. S. Bullock, T. S. Kolatt, Y. Sigad, R. S. Somerville, A. V. Kravtsov, A. A. Klypin, J. R. Primack, A. Dekel, *Mon. Not. R. Astron. Soc.* **321**, 559 (2001).

- [23] V. Berezhinsky *et al.*, Phys. Lett. B **294**, 221 (1992).
- [24] X. J. Bi, Nucl. Phys. B **741**, 83 (2006); X.-J. Bi, Y.-Q. Guo, H.-B. Hu, X. Zhang, Nucl. Phys. B **775**, 143 (2007).
- [25] A. W. Strong, I. V. Moskalenko, Astrophys. J. **509**, 212 (1998);
- [26] A. J. Davis *et al.*, AIP Conf. Proc. 528, (2000), eds. R. A. Mewaldt *et al.* (New York: AIP), 421.
- [27] M. A. DuVernois, J. A. Simpson, M. R. Thayer, Astron. Astrophysics **316**, 555 (1996).
- [28] A. Lukasiak, F. B. McDonald, W. R. Webber, Proc. 26th Int. Cosmic Ray Conf. (Salt Lake City), 3, 41 (1999).
- [29] J. J. Engelmann, P. Ferrando, A. Soutoul, P. Goret, E. Juliusson, Astron. Astrophysics **233**, 96 (1990).
- [30] J. H. Chapell, & W. R. Webber, Proc. 17th Int. Cosmic Ray Conf. (Paris), 2, 59 (1981); R. Dwyer, Astrophys. J. **224**, 691 (1978); R. C. Maehl, J. F. Ormes, A. J. Fisher, & F. A. Hagen, Ap&SS, 47, 163 (1977).
- [31] J. J. Connell, Astrophys. J. **501**, L59 (1998).
- [32] N. E. Yanasak *et al.*, Proc. Symp. ACE-2000, AIP (2000); W. R. Binns *et al.*, Proc. 26th Int. Cosmic Ray Conf. 3, 21, (1999).
- [33] A. Lukasiak, F. B. McDonald, W. R. Webber, Proc. 26th Int. Cosmic Ray Conf. OG 1.1.12 (1999)
- [34] T. Sanuki *et al.*, Astrophys. J. **545**, 1135 (2000).
- [35] J. Alcaraz *et al.*, Phys. Lett. B **490**, 27 (2000)
- [36] M. Boezio *et al.*, Astrophys. J. **532**, 653 (2000).
- [37] S. W. Barwick *et al.*, Astrophys. J. **498**, 779 (1998).
- [38] A. W. Strong, I. V. Moskalenko, O. Reimer, S. Digel, R. Diehl, Astron. Astrophys. **422**, L47 (2004).
- [39] T.J. Sodroski *et al.*, Astrophys. J. **480**, 173 (1997).
- [40] A. Boselli, J. Lequeux, G. Gavazzi, Astron. Astrophys. **384**, 33 (2002).
- [41] A. W. Strong, J. R. Mattox, Astron. Astrophys. **308**, L21 (1996).
- [42] D. R. Lorimer, *Young Neutron Stars and Their Environments*, IAU Symposium, Vol.218 (2004).
- [43] Gary L. Case & Dipen Bhattacharya, Astrophys. J. **504**, 761 (1998).

- [44] G. Basini *et al.*, Proc. 26th Int. Cosmic Ray Conf. 3, 77 (1999)
- [45] M. Boezio *et al.*, Astrophys. J. **561**, 787 (2001).
- [46] S. Orito *et al.*, Phys. Rev. Lett. **84**, 1078 (2000).
- [47] T. Maeno *et al.*, Astropart. Phys. **16**, 121 (2001).
- [48] Asaoka *et al.*, Phys. Rev. Lett. **88**, 051101 (2002).
- [49] Haino *et al.*, Proc. 29th Int. Cosmic Ray Conf. 3, 13 (2005).
- [50] Aguilar *et al.*, Physics Reports 366, 331 (2002)
- [51] I. V. Moskalenko, A. W. Strong, J. F. Ormes, M. S. Potgieter, Astrophys. J. **565**, 280 (2002);
I. V. Moskalenko, A. W. Strong, S. G. Mashnik, J. F. Ormes, Astrophys. J. **586**, 1050 (2003).
- [52] F. Donato, N. Fornengo, D. Maurin, P. Salati, R. Taillet, Phys. Rev. D**69**, 063501 (2004).
- [53] A. W. Strong I. V. Moskalenko, Adv. Space Res. **27**, 717 (2001).
- [54] D. Maurin, F. Donato, R. Taillet, P. Salati, Astrophys. J. **555**, 585 (2001).
- [55] D. Maurin, R. Taillet, F. Donato, Astron. Astrophys. **394**,1039 (2002).
- [56] Thomas K. Gaisser, "*Cosmic Rays and Particle Physics*", Cambridge University Press, (1990)
- [57] B. D. G. Chandran, Space Sci.Rev. 99, 271 (2001)
- [58] http://statistics.roma2.infn.it/~scineghe07/talks/grasso_scineghe07.pdf.
- [59] A. Lyne & F. Graham-Smith, "*Pulsar Astronomy*", 3rd Edition, Cambridge University Press (2005).
- [60] P.M.W. Kalberla, L. Dedes, J. Kerp, U. Haud, arXiv:0704.3925
- [61] see <http://wizard.roma2.infn.it/pamela/>
- [62] see <http://ams.cern.ch/>
- [63] W. de Boer, I. Gebauer, C. Sander, M. Weber, V. Zhukov, astro-ph/0612462; I. Gebauer, arXiv:0710.4966.
- [64] D. Maurin, R. Taillet, C. Combet, astro-ph/0609522v3; D. Maurin, R. Taillet, C. Combet, astro-ph/0612714v1; J. Lavalle, Q. Yuan, D. Maurin, X. J. Bi, Astron. Astrophys. **479**, 427 (2008).
- [65] F. W. Stecker, S. D. Hunter, D. A. Kniffen, arXiv:0705.4311
- [66] see <http://www-glast.stanford.edu/>





PARTICLE SPECTRA: positrons

